The Probable Metapelite Nature of Sapphirine–Spinel and Garnet Gedritites of the Aulandzha Block of the Omolon Massif

O.V. Avchenko[a], K.V. Chudnenko[b]

*[a] Far East Geological Institute, Far Eastern Branch of the Russian Academy of Sciences,
pr. 100 Let Vladivostoku 159, Vladivostok, 690022, Russia*

*[b] A.P. Vinogradov Institute of Geochemistry, Siberian Branch of the Russian Academy of Sciences,
ul. Favorskogo 1a, Irkutsk, 664033, Russia*

Abstract—Unique magnesian–aluminous ultrabasic sapphirine–spinel and garnet gedritites of the Aulandzha block were studied. The deepest part of the Archean Stage of the Omolon massif is exposed in this district. The gedritites differ strongly in petrochemistry and geochemistry from other metaultramafites of this block. The difference is in their enrichment in alumina, zirconium, barium, rubidium, hafnium, and uranium and depletion in calcium and heavy rare-earth elements. The oxidizing potential in the sapphirine–spinel assemblage, estimated by physicochemical modeling, showed high oxygen fugacity in these rocks, close to the value of the magnetite–hematite buffer, which was never observed in ancient granulite complexes. The above petro- and geochemical features of the gedritites of the Aulandzha block, having an isotopic age of 1.9 Ga, are explained by the fact that these rocks are probably the crust of weathering of the enclosing metaultramafites. If this hypothesis is true, then the above rocks may indicate that the oxygen potential on the Earth's surface corresponded to the magnetite–hematite buffer as early as the Paleoproterozoic.

Keywords: gedritites, sapphirine, metaultramafites, crust of weathering, oxidizing potential, Paleoproterozoic metamorphism, Omolon massif, Northeastern Asia

INTRODUCTION

Among the garnet metaultramafites of the Omolon massif I.L. Zhulanova found unique rocks containing gedrite and sapphirine, which is a single finding of these minerals in the Precambrian complexes of Northeast Asia. In addition, the value of these rocks is defined by the fact that a detailed isotope–geochemical study of the zircons was performed in them (Akinin and Zhulanova, 2016). In the cited publication it is shown that the most reliable dating is the Paleoproterozoic age of 1.9 Ga, recorded in the transparent rims of the large zircon crystals and in its newly formed fine grains. At the same time, in the cores of the large zircon crystals with oscillatory zoning a Paleoarchean age (3.4–3.2 Ga) was determined. This paper is devoted to the analysis of the genesis of these rocks, which, as the investigations showed, is not uniquely metamagmatic but bears the evidence of metasedimentary (or metapelitic) nature. In turn, the available factual and calculation material showed that the recognition of the metasedimentary nature allows making a conclusion about a possible value of the oxygen potential on the Earth's surface

during the formation of these rocks. The petrology of these samples was discussed in detail in the paper (Avchenko et al., 2018).

GEOLOGICAL POSITION OF GARNET METAULTRAMAFITES

The Omolon massif (OM) is marked by the longest evolution compared to other tectonic elements of the modern continent–ocean transition zone in Northeast Asia. In its structure, the ancient crystalline basement and poorly deformed Riphean–Mesozoic volcanosedimentary cover are clearly distinguished. Today the OM is more often considered a craton terrane or microcontinent. The complicated and many-stage history of the development of the pre-Riphean crystalline basement of the OM, the outcrops of which are concentrated in south of terrane, was established (Gel'man, 1974; Bibikova, 1989). Of special interest is the Aulandzha block (horst, protrusion), where the deepest part of the Archean continental crust of the Verhoyansk–Chukotka region is exposed.

Within the Aulandzha block (about 350 km^2) a fragment of the dome (western part) is reconstructed, the core of which is composed of charnockitoids (Fig. 1). As the relicts of the substratum, the amphibole–bipyroxene schists, some-

✉Corresponding author.
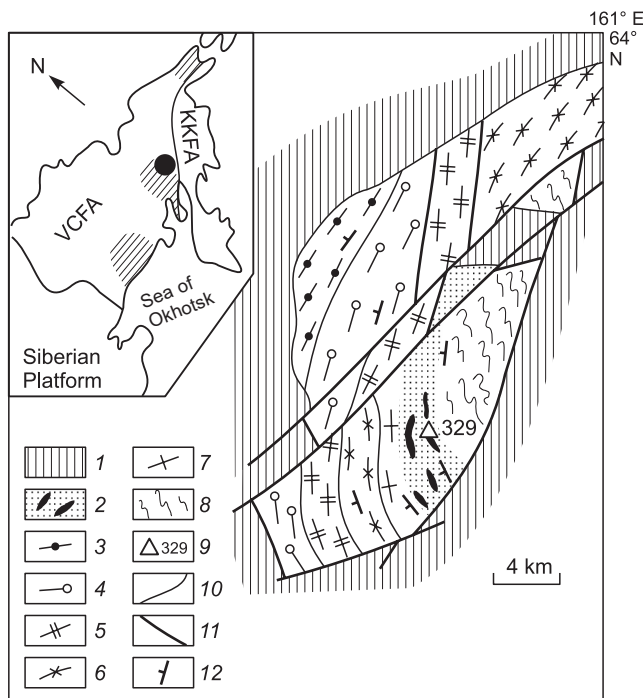 *E-mail address:* sirenevka@mail.ru (O.V. Avchenko)

Fig. 1. Schematic geological map of the Aulandzha protrusion of the basement of the Omolon massif. Compiled by I.L. Zhulanova (1990). *1*, Riphean and Paleozoic sedimentary deposits; *2–8*, Lower Archean: *2*, biotite granite-gneiss with lenses of garnet metaultramafites; *3*, garnet–biotite plagiogneisses, biotite–hypersthene schists; *4*, diopside plagiogneisses, bipyroxene–amphibole schists, garnet–biotite gneisses; *5*, amphibolites, diopside–amphibole schists; *6*, predominantly garnet–biotite gneisses, sometimes cordierite-bearing ones; *7*, diopside amphibolites, bipyroxene–amphibole and garnet–diopside–amphibole schists; *8*, charnockitoids, amphibole–bipyroxene schists, leucocratic granulites; *9*, location of garnet and sapphirine gedritites, number of the observation point; *10*, geological boundaries; *11*, faults; *12*, attitude of the banding of metamorphic rocks. In the insert: shaded zones show districts of occurrence of the outcrops of the pre-Riphean metamorphic formations in the Verhoyansk–Chukotka folded region (from southwest to northeast: Okhotsk, Omolon–Taigonos, and East Chukotka). VCFA, Mesozoic Verhoyansk–Chukotka folded area. KKFA, Cenozoic Koryak–Kamchatka folded area. Black circle indicates the location of the Aulandzha protrusion.

times with garnet, are observed universally, and leucocratic granulites are rare. On the limb, the stratified section is stripped, which is dominated by Ca-rich mesocratic gneisses, schists (including bipyroxene ones), and amphibolites, the alternation of which with one another and with the aluminous masses answers the criteria of the premetamorphic lamination. The garnet metaultramafites compose lenslike bodies 5 to 50 m thick inside a wide (4–5 km) band of the biotite granite-gneisses cementing the zone of the nonevident disconformity between the core and limb of the dome. The chains of the melanocratic bodies, traced for a distance of ~5 km, approach in space the dome core and fit conformably in its general structure. They are interpreted as the fragments (tectonic detached masses) of the foot of the charnockitoid antiform (Kotlyar et al., 2001).

Some bodies differ from each other in structure (massive or banded; the width of the bands is from the first millimeters to several decimeters), quantitative ratio of the main minerals and their sizes (fine- or medium-grained, more rarely porphyroblastic owing to the evenly distributed garnet grains up to 10 mm across), and the presence of accessory minerals (biotite, ilmenite, etc.). The petrotype includes the medium-grained varieties of the granoblastic structure composed of garnet, clinopyroxene, and brown hornblende approximately in equal ratios with the admixture of orthopyroxene (5–8%). The garnet-free bipyroxene–hornblende (the orthopyroxene content is up to 20%) and clinopyroxene–hornblende rocks occur rarely.

In a single case, in the band of the garnet metaultramafite outcrops (Bol'shaya Aulandzha–Anmandzha River divide), there was a lens-shaped bedrock body (8 × 20 m) demonstrating the coarse- and giant-grained texture, sharp textural heterogeneity, and absence of schistosity. Deep red garnet porphyroblasts 2–3 to 80 mm in size, unevenly distributed in the rock mass, stand out sharply against the hornblende that forms aggregates of differently oriented black shiny crystals up to 15 mm across. Their main groundmass is characterized by a coarse-taxite structure (accumulations of hornblende of the irregular form, concretions and veinlets of the coarse-grained white, sometimes with a greenish tint, plagioclase, small nests of biotite, etc.), but in the general orientation inside the enclosing body the subparallelism is seen. In the main substance of one of the lenses, in its inner part, free of large garnet porphyroblasts, there were medium-grained segregation (up to 7 cm across and up to 10 cm long) of greenish gray color that from the laboratory investigations were classified as garnet gedritites. The lower margin of this lens is rimmed by a symmetrically-banded aggregate (6–8 cm thick and about 30 cm long) with visible alternation of the goldish brown bands rich in gedrite (3–5 to 10–15 mm wide) and gray-blue essentially plagioclase ones (3–8 mm wide). The texture of the aggregate described resembles the bedding of a sedimentary rock (Fig. 2). In addition, sapphirine, biotite, orthopyroxene, and relics of green spinel inside the sapphirine segregation were found in thin sections. These rocks are described below as the sapphirine–spinel gedritites. The geographical coordinates for the studied samples according to the data by Zhulanova (1990) are given in Table 1.

Table 1. Geographical coordinates of the studied samples from data of Zhulanova (1990)

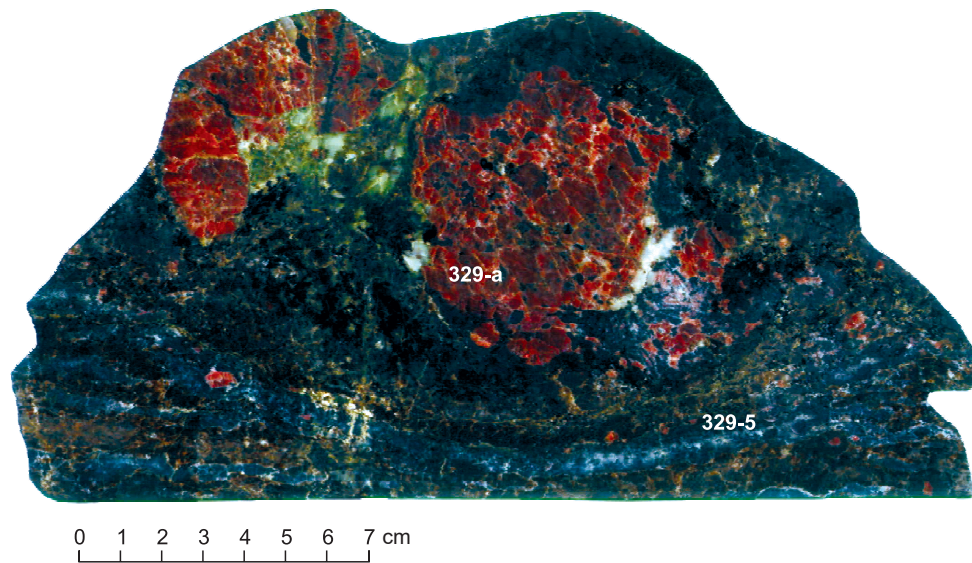| Sample no.	Coordinates	
	N	E
325	63°41′00″	160°47′40″
325-zh	63°41′20″	160°48′30″
327	63°42′00″	160°50′30″
a-339	63°42′20″	160°47′10″
329-a	63°42′20″	160°47′40″
329-5	63°42′20″	160°47′40″

0 1 2 3 4 5 6 7 cm

Fig. 2. Lenslike separation of garnet (sample 329-a) and banded sapphirine–spinel (sample 329-5) gedritites in the ultramafite body of the Auland-zha block.

ANALYTICAL INVESTIGATIONS

The rock and mineral composition was analyzed at the Analytical Center of the Far East Geological Institute, Far Eastern Branch of the Russian Academy of Sciences. The chemical analysis of minerals was done using the JXA 8100 four-channel microanalyzer. The contents of the petrogenic components in rocks were estimated by ICP AES using the iCAP 6500 Duo spectrometer. The contents of H_2O^-, LOI, and SiO_2 were determined with the method of gravimetry. The minor elements were defined by ICP MS using the Agilent 7500 c spectrometer (Agilent Technologies, United States). The samples were prepared by lithium metaborate fusion. The thin and polished sections were studied at the laboratories of the electron and light microscopy of the Analytical Center of the Far East Geological Institute equipped with the modern Carl Zeiss (AXIOPLAN 2 and AXIOSTAR plus) and LOMO (POLAM R-213) high-precision light microscopes.

PETROGRAPHY OF THE SAPPHIRINE–SPINEL AND GARNET GEDRITITES

The sapphirine–spinel gedritite (sample 329-5, Fig. 2) is composed of (in decreasing order) gedrite, plagioclase, biotite, orthopyroxene, sapphirine, and spinel. The texture is granonematoblastic heterograined with the areas of the mosaic one, and the structure is thin-banded. The sapphirine and spinel demonstrate the effective reactional interrelations: The greenish blue sapphirine with the clear pleochroism surrounds in full the dark green spinel, so that its segregations begin to look like peculiar cores (relicts). They are

observed in most (but not in all) crystals of sapphirine whose individuals vary from 0.2 to 0.6 mm in length (Fig. 3).

The spinel–sapphirine intergrowths elongate into chains along the axis of the plagioclase bands, which are 2–3 mm wide and are divided at the least in half by wider bands dominated by the dark-colored minerals. The plagioclase
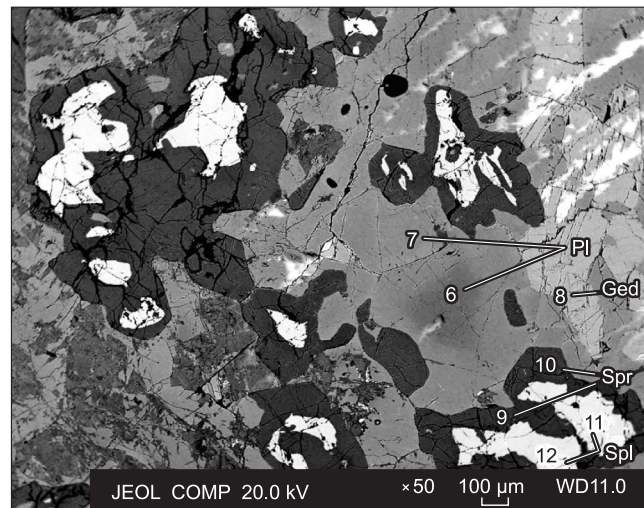

Fig. 3. Back-scattered electron image of rims of sapphirine (black) around spinel (white), sample 329-5. Numbers in the figure are points of analyses of minerals given in Table 4 in the paper (Avchenko et al., 2018): 6, the core of a zoned crystal of plagioclase (61% An); 7, outer zones of a zoned crystal of plagioclase (75% An); 8, gedrite; 9,10, sapphirine; 11,12, spinel. Mineral name abbreviations are after Whitney and Evans (2010). Hereinafter: Spr, sapphirine; Spl, spinel; Bt, biotite; Opx, orthopyroxene; Pl, plagioclase; Grt, garnet; Hem, hematite; Mag, magnetite; Ged, gedrite.

bands represent a mosaic aggregate of isometric grains (0.5–1.0 mm) contacting mostly along the straight-line boundaries, often with the formation of the regular triple joints. Polysynthetic twins and reverse zoning with smooth transitions between the zones are common. Muscovitization is observed on small areas and along the cleavage cracks.

In the dark bands the largest separations belong to gedrite. Its subeuhedral and strongly elongated (1–3 × 5–8 mm) crystals are evenly colored in the characteristic light brown color with the clear pleochroismare confined to the boundaries of the plagioclase bands and are localized along them. The smaller ones are oriented randomly. The same structural position is shown by biotite composing no less than 5–6% of the rock volume. It forms narrow long well-crystallized plates of bright red-brown color with sharp pleochroism; in places it accumulates in the monomineral bands of the same structural direction. Orthopyroxene is observed only as thin-structural symplectic intergrowths with plagioclase between the large crystals of gedrite.

On the periphery of the thin-banded aggregate, in the zone of its contact with the coarse-taxite part of the garnet–hornblende lens, there are fine garnet grains, whose irregular form and resorbed boundaries testify to their relict nature. In the thin sections one can see that on the margins of such grains the large subeuhedral crystals of gedrite grow, which contain the regularly oriented and relatively large wormlike ingrowths of plagioclase (diablastic texture). The chemical composition of the minerals and their crystallochemical formulas are given in the paper (Avchenko et al., 2018). The analyses confirm the strong reverse zoning of plagioclase: The crystal cores are composed of labradorite, and the rims consist of bytownite (56–61 and up to 75–80% An, respectively). On the photographs in the reflected electrons, the relatively acidic zones are marked by a darker color (Fig. 3). Sapphirine shows a high magnesium content X_{mg} (Mg/(Mg + Fe^{2+})) and high oxidation degree $X_{Fe^{3+}}$ (Fe^{3+}/(Fe^{3+} + Fe^{2+})): X_{mg} = 0.88–0.91; $X_{Fe^{3+}}$ = 0.31–0.53. Spinels coexisting with sapphirine are less magnesian and less oxidized: X_{mg} = 0.63–0.65; $X_{Fe^{3+}}$ = 0.13–0.20 (a similar regularity was noted by L.M. Kriegsman and J.C. Schumacher (1999)). The sapphirine gedrite (sample 329-5) is composed of the mineral assemblages of several generations, but the unique segregation of the equilibrium phases is a rather difficult problem. We think that the latest generation is composed of biotite, gedrite, sapphirine, and surrounding zones of the basic plagioclase. Spinel is by far the earliest one relatively to sapphirine, but the judgement about the minerals coexisting in equilibrium with it before the sapphirine originated requires the further study.

Garnet gedritite (sample 329-a, Fig. 2) is composed of garnet, plagioclase, orthopyroxene, gedrite, and biotite. The texture is granoblastic heterograined, and the structure is massive taxitic. Around the garnet porphyroblasts (10–15 mm) reaction rims are visible to the naked eye. Under the microscope it is seen that they are present almost in all gar-

net segregations. They differ in the mineral composition and features of the inner structure: from the narrow orthopyroxene–plagioclase and wider gedrite–orthopyroxene–plagioclase to full pseudomorphs composed of the fine-structure symplectite of plagioclase, hypersthene, and gedrite.

The analytical investigations were done in the area where the rounded garnet grain about 1 cm across is surrounded by the symplectite of orthopyroxene and plagioclase with an average size of individuals of 0.05 × 1.00 mm, to which the small subeuhedral segregations of gedrite join closely. All analyses of minerals and their crystallochemical formulas are given in the paper (Avchenko et al., 2018).

The minerals show the chemical zoning, which is best pronounced in plagioclase. Small segregations in the reactional rims are composed of bytownite (up to 87% An), and the grains at a distance from garnet show reverse zoning: the core is labradorite, and the periphery is bytownite (55–59 and 75–81% An, respectively). Garnet as a whole has a low iron content (X_{Fe}^{Gr} = Fe/(Fe + Mg)) that increases from center to margins from 0.43 to 0.51. In the orthopyroxene the iron content varies insignificantly (0.27–0.28), but the alumina content (Al$_2$O$_3$, wt.%) in the rims is somewhat higher (6.3–6.4) than it is at a distance from them (5.0–5.7). The composition of gedrite and biotite is almost constant. Gedrite belongs to the sodic group, which, according to (Berg, 1985), must have Na^A f.u. ≥0.5 at Mg/(Mg + Fe^{+2}) ≥ 0.50. In our analyses these parameters are 0.6 and ≥0.7, respectively. Biotite has a low iron content (X_{Fe}^{Bi} = 0.22–0.21).

All this data indicate that two generations of minerals can be distinguished in sample 329-a: the early generation (magnesian garnet, labrador, and orthopyroxene with a low alumina content) and the late generation (garnet with a high iron content and the minerals replacing it: bytownite, aluminous orthopyroxene, and gedrite). The study of the interrelations of the crystals of gedrite and plagioclase allows the obvious conclusion that gedrite always contacts only the basic plagioclase marginal zones, which shows to its superposition on the early assemblages.

FEATURES OF PETROCHEMISTRY AND GEOCHEMISTRY OF SAPPHIRINE–SPINEL AND GARNET GEDRITITES

The chemical composition of the sapphirine–spinel and garnet gedritites is similar as a whole, but the sapphirine–spinel gedritites differ from the garnet ones in a higher content of alumina (24.67 against 18.37 wt.%) and K$_2$O (2.03 against 1.51 wt.%) (Table 2). As for the CaO and Al$_2$O$_3$ components, both varieties of gedritites strongly differ from the enclosing metaultramafites: Gedritites are enriched in alumina and contain much less calcium, so that on the CaO–Al$_2$O$_3$–K$_2$O triple diagram they form an individual group as compared with the metaultramafites (Fig. 4; Table 2). At the same time, on the TAS diagram for classification of igneous

Table 2. Chemical (wt.%) and trace-element (ppm) composition of metaultramafites of the Aulandzha block of the Omolon massif

Component	325	325-zh	327	a-339	329-a	329-5
SiO_2	47.50	47.10	42.50	43.45	44.70	43.95
TiO_2	1.05	1.36	1.09	0.94	1.09	0.48
Al_2O_3	7.16	13.50	15.39	15.57	18.37	24.67
Fe_2O_3	3.38	5.88	2.96	4.49	2.87	7.04
FeO	10.52	11.13	10.47	11.00	10.25	N.d.
MnO	0.211	0.287	0.125	0.264	0.220	0.04
MgO	19.43	6.78	11.13	10.35	14.21	12.65
CaO	7.30	10.93	12.62	12.59	5.32	4.81
Na_2O	1.27	2.26	1.45	1.21	1.20	1.52
K_2O	0.66	0.42	0.67	0.29	1.51	2.03
P_2O_5	0.11	0.12	0.11	0.06	0.04	0.02
LOI	0.98	0.61	1.08	0.26	0.70	2.25
Total	99.58	100.37	99.57	100.48	100.49	99.56
Rb	10.71	3.69	11.94	1.47	43.24	86.41
Zr	121.3	62.70	39.16	23.03	567.5	366.5
Cs	0.17	0.10	0.17	0.08	0.32	1.04
Ba	157.8	86.90	98.10	29.09	315.5	323.9
La	12.17	10.09	4.95	4.07	8.87	2.6
Ce	28.83	22.74	11.99	9.38	28.18	7.05
Pr	3.32	2.86	1.80	1.37	4.65	1.9
Nd	14.83	12.98	9.53	7.17	25.70	12.77
Sm	3.66	3.72	3.20	2.33	7.11	5.76
Eu	1.02	1.22	1.10	0.81	1.63	1.35
Gd	3.88	4.43	4.09	3.24	7.00	6.2
Tb	0.64	0.84	0.74	0.61	0.91	0.88
Dy	3.73	5.53	4.56	3.98	4.68	4.07
Ho	0.68	1.21	0.95	0.88	0.77	0.6
Hf	2.82	1.81	1.20	0.72	12.73	8.43
U	0.17	0.33	0.11	0.06	0.54	0.39

Note. The H_2O^-, LOI, and SiO_2 contents were determined with the method of gravimetry, analyst V.N. Zalevskaya. The content of the rock-forming components was determined by ICP AES on the iCAP 6500 Duo spectrometer (Thermo Electron Corporation, United States), and trace elements were determined by ICP MS on the Agilent 7500 c spectrometer (Agilent Technologies, United States), analysts M.G. Blokhin, G.A. Gorbach, E.A. Tkalina, and N.V. Khurkalo. Sample preparation was done by lithium metaborate fusion. Analyst L.S. Levchuk. Responsible executor N.V. Zarubina.

rocks (Sharpenok, 2009), all the samples fall in the fields of basic and ultrabasic moderately alkali picrobasalts (Fig. 5).

Very peculiar is the geochemistry of gedritites. As compared with other metaultramafites the sapphirine and garnet gedritites are enriched in Zr, Ba, Rb, Hf, and U (Table 2). Their specific character is especially pronounced on the Zr–Ba and Zr–Rb diagrams (Fig. 6). The figurative points of samples 329-a and 329-5 are significantly remote from those of all the other samples of the metaultramafites grouped near zero. The attention is first of all directed to high contents of Zr in gedritites, which is reflected in the contamination of these rocks with the zircon crystals of different sizes. Such

Table 3. Average content of Zr (ppm) in rocks of the Earth's crust, after (Kogarko et al., 1988)

Rocks	Zr, ppm
Ultrabasite	34
Ultrabasites from alkaline intusions	106
Basites	50
Alkali gabbro	142
Intermediate	150
Acidic	200
Basic	104
Tholeiitic basalts	100
Tholeiitic basalts of oceanic islands	200
Alkali syenites	510
Alkali granites	837

Zr contents are quite unusual for the ultrabasic rocks (Table 3). The differences of the geochemistry of the sapphirine–spinel and garnet gedritites from that of the enclosing metaultramafites are observed also in the field of the REE contents. The REE patterns of the metaultramafites show that the sapphirine–spinel and garnet gedritites are rather depleted in heavy REE as compared with other metaultramafites (Fig. 7).

THERMOBAROMETRY OF SAPPHIRINE–SPINEL AND GARNET GEDRITITES

To calculate the thermodynamic parameters of the formation of two same-named but different-time mineral assemblages of garnet + orthopyroxene + plagioclase, defined in garnet gedritites (sample 329-a), we initially (Zhulanova et al., 2014) used the experimental instruments: geobarometer of A.A. Grafchikov and V.I. Fonarev (1991) and garnet–orthopyroxene geothermometer of I.L. Lavrent'eva and
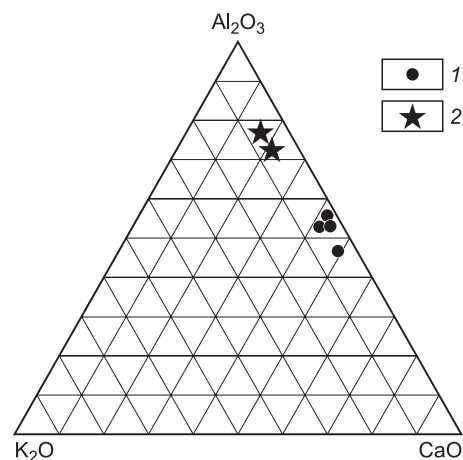
Fig. 4. Position of the figurative points of metaultramafites of the Aulandzha block on the $CaO–K_2O–Al_2O_3$ triple diagram. *1*, typomorphic metaultramafites (samples a-339, 327, 325-zh, and 325); *2*, garnet (329-a) and sapphirine (329-5) gedritites.
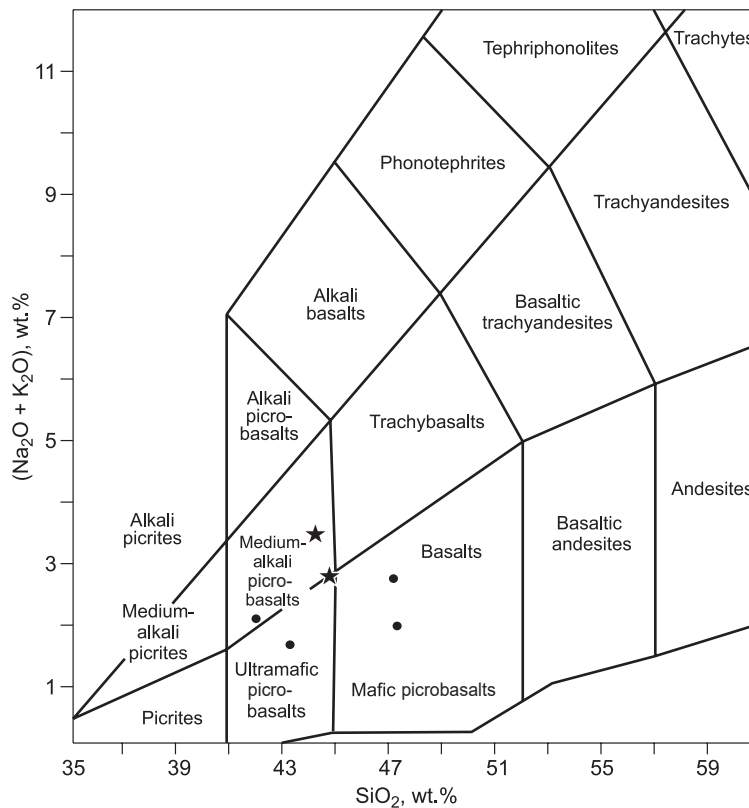
Fig. 5. Position of figurative points of metaultramafites on the TAS diagram (Sharpenok, 2009). See legend in Fig. 4.

L.L. Perchuk (1991). According to the refined data, the relatively earlier association, which characterizes garnet metaultramafites, was formed under conditions of the granulitic facies of the higher pressures ($T = 860$ °C; $P = 9$ kbar), and the later one answers the amphibolitic facies and marks the stage of decompression accompanied by a significant decrease of temperature ($T = 650$ °C; $P = 5.5$ kbar). However, the geobarometer of Grafchikov and Fonarev is intended for the assemblages which contain quartz in addition to garnet, orthopyroxene, and plagioclase. If quartz is absent in the mineral assemblage (as it is in our case), then the estimate of the pressure can be too high. Thus, for the early assemblage, $P < 9$ kbar, and for the late one, $P < 5.5$ kbar.

L.Ya. Aranovich with the TWQ version, improved by him, in which the garnet–orthopyroxene thermobarometer is fitted (Aranovich and Berman, 1997), obtained the correlated estimates for sample 329-a: $T = 840$ °C; $P = 4.8$ kbar (analyses 1–9 in Table 1; Avchenko et al., 2018). Other mineral compositions with TWQ did not give good intersections. The temperature of the garnet–orthopyroxene equilibrium of 840 °C almost coincides with the temperature of 842 °C, if it is calculated from the same analyses of minerals for 5 kbar with the garnet–orthopyroxene geothermometer of Lavrent'eva and Perchuk (1991). When judging from the position of the points of analyses of minerals in sample 329-a (Fig. 2, Avchenko et al., 2018), then these estimates of the temperature and pressure are restricted to the stage of origi-

nation of the reactional structures in this sample. As for the probable temperatures of the early and late mineral assemblages in sample 329-a, of interest are the temperatures of crystallization of zircons from the garnet gedritites calculated from the Ti concentrations (Ferry and Watson, 2007). They fall in the 760 to 880 °C interval, and in the zircon cores the temperatures are systematically higher than those in the rims with the maximal temperature of 940 °C (Akinin and Zhulanova, 2016). For sample 329-5 the temperature of the sapphirine–spinel equilibrium can be determined with the available thermometers. With the experimental sapphirine–spinel thermometers the equilibrium temperature is determined as 780 °C (Sato et al., 2006) and 994 °C (Das et al., 2006), and with the empiric sapphirine–spinel thermometer (Owen and Greenough, 1991) the temperature of the sapphirine–spinel equilibrium is 861 °C. The correlation shows that the empiric sapphirine–spinel thermometer corresponds well to the determinations of temperatures with TWQ and garnet–orthopyroxene thermometer. The experimental sapphirine–spinel thermometers appear to be less accurate, because they do not account for the oxidation degree of iron in sapphirine. Evidently, one can assume that the reactional structures in samples 329-a (gedrite–orthopyroxene–plagioclase intergrowths around garnet) and 329-5 (sapphirine rims around spinel) originated at pressure of about 5 kbar and temperatures of 840–860 °C. In the paper (Avchenko et al., 2018) the origination of the reactional structures is con-
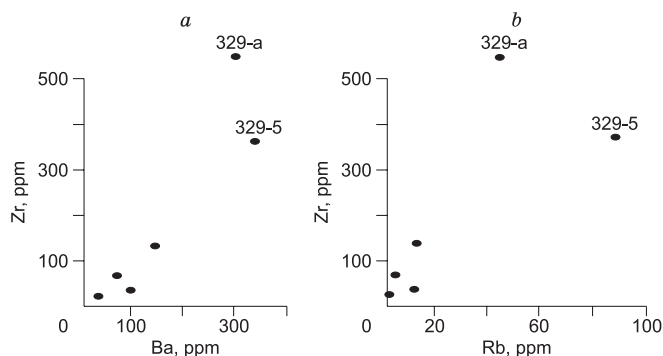
Fig. 6. Diagrams of the Zr–Ba (*a*) and Zr–Rb (*b*) ratios in the typomorphic metaultramafites (samples a-339, 327, 325-zh, and 325) and garnet (sample 329-a) and sapphirine (sample 329-5) gedritites (Aulandzha block).

Fig. 7. Distribution of the REE contents in the metaultramafites of the Aulandzha block, normalized to chondrite (McDonough and Sun, 1995).

sidered to be connected with the metamorphism evolution along the regressive *P*–*T* trend from the peak conditions of metamorphism (*P* = 7 kbar; *T* = 1000 °C) to the conditions of the reactional structure formation with further decrease of temperature and pressure under conditions of the classic amphibolite facies (Fig. 8). This *P*–*T* trend was obtained from the calculations with the TWQ, thermometrical data on zircon, modeling on the Selector software, and extrapolation under conditions of the formation of spinel granulites.

CONDITIONS OF FORMATION OF SAPPHIRINE–SPINEL REACTIONAL STRUCTURES FROM OXIDATION POTENTIAL

As it will be seen from further discussion, the prime consideration for this paper is the evaluation of the oxygen potential in the sapphirine–spinel assemblage. We will discuss in detail the methods of evaluation of the oxygen potential in this paragenesis with the method of modeling, as it is impossible to solve this task with the method of the stoichiometric formalism accepted in petrology.

It was established long ago that significant amounts of the trivalent iron can be present in the sapphirine structure (Steffen et al., 1984). For example, the maximal content of the trivalent iron in sapphirine from the Mössbauer spectra at temperature of 1100 °C and pressure 2 kbar can reach 0.7 for a crystallochemical formula. Thus, the sapphirine composition can serve as a potential oxygen meter, and the calculation of the sapphirine-bearing phase diagrams must be done with the account of the trivalent iron. However, only in 2010 did researchers try to add the trivalent iron into the model of the solid solution of sapphirine (Taylor-Jones and Powell, 2010). It was improved in (Wheller and Powell, 2014) and correlated with the refined thermodynamic data of the end-members published in (Holland and Powell, 1998, 2011). This model and corresponding thermodynamic data of the end-members were inserted into the Selector software and served as the base for the calculation of the oxygen potential in the sapphirine–spinel assemblages.
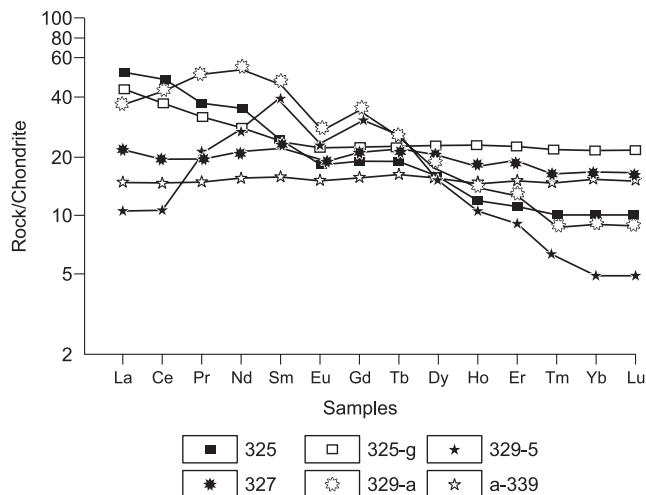
Modeling using the Selector software is based on a certain chemical composition of the rock (Avchenko et al., 2009). For this purpose we took the real composition of sample 329-5 (Table 2), which we inserted into the task. We used the two-reservoir model, when a fluid is placed into one reservoir, and a given composition of the rock is placed into the other. In the process of modeling the fluid of a cer-
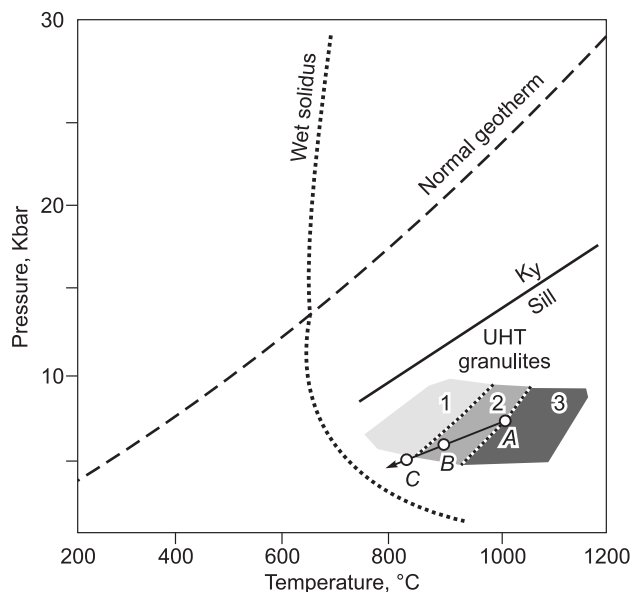

Fig. 8. Probable *P*–*T* trend of the metamorphism evolution of the Aulandzha protrusion. Points *B* and *C* were calculated using the garnet–orthopyroxene geobarothermometer embedded into the TWQ program (point *C*) and on the basis of modeling of sample 329-5 (point *B*). Point *A* is the extrapolation of the *BC* line in the field of the spinel granulites. UHT is a field of the ultrahigh-temperature granulites (Kelsey and Hand, 2015). 1–3, fields of parageneses calculated with the Selector software on the basis of sample 329-5: 1, with sapphirine and without spinel; 2, with sapphirine and spinel; 3, with spinel and without sapphirine.

tain composition passes into the reservoir where the rock is localized, and there the reaction occurs with the formation of the equilibrium paragenesis and corresponding fluid. The solution contains the mineral and fluid compositions. The modeling was done with the use of the thermodynamic base (Holland and Powell, 1998) with regard to the models of solid solutions. As compared with the book (Avchenko et al., 2009) the database on the models of solid solutions was essentially reworked and widened due to new models of the ortho- and clinoamphiboles, biotite, clinopyroxene, ilmenite, spinel, and sapphirine published in the papers (White et al., 2002, 2005; Diener et al., 2007; Green et al., 2007; Tajčmanová et al., 2009).

A gas fluid was modeled with an ideal mixture of the H_2O, CO_2, CH_4, CO, H_2, and O_2 real gases, and the dependence of the gas thermodynamic characteristics on the pressure was calculated using the Benedict–Webb–Rubin equation of state, modified by B.I. Lee and M.G. Kesler (1975). Then under conditions of buffering of fluid with the considered rock (sample 329-5) we searched for such P and T conditions that the solution results in the model assemblage containing sapphirine and spinel, and the mineral compositions in it would be maximally close to those observed in reality. As it turned out, at $P = 6$ kbar and $T = 900$ °C and with a quite certain fluid composition one can create the mineral assemblage containing sapphirine and spinel whose compositions are very similar in the magnesium content and oxidation degree to the compositions observed in reality (Table 4). It should be noted that the obtained model parameters of P and T are rather close to the P and T estimates obtained with the geothermobarometers. The solution makes it possible to obtain the value of the oxygen activity (fugacity) in the given mineral assemblage. The parameters of the fluid composition before and after the reaction with the rock are given in Table 5. The calculations showed that the value of the oxygen fugacity logarithm in the originated Spr + Spl + Pl + Opx + Bt + Grt model assemblage (see Fig. 3 for mineral indices) at 900 °C and 6 kbar turned out to be –8.7, and $\lg f_{O_2}$ on the magnetite–hematite (MagHem) buffer at the same P and T parameters is –8.4 (Fig. 9). A whole set of the careful earlier measurements of the oxygen activity in the rocks of the granulite facies of the Sutam complex
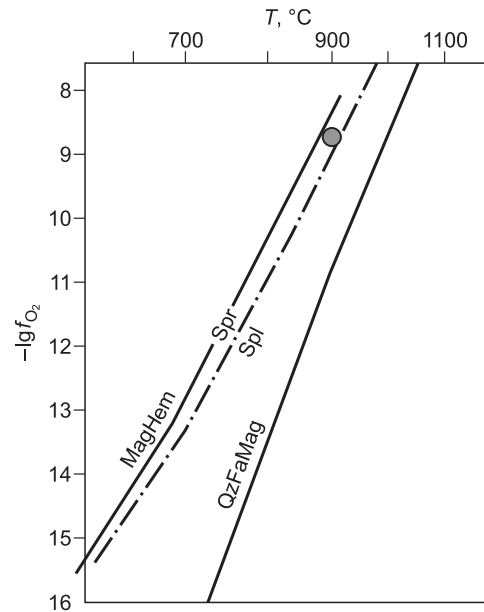

Fig. 9. Value of the oxygen activity in the sapphirine–spinel assemblage (circle) for sample 329-5 on the $\lg f_{O_2}$–T diagram, $P = 6$ kbar. Solid lines show the magnetite–hematite (MagHem) and quartz–fayalite–magnetite (QzFaMag) buffer equilibria; dash-and-dot line marks the boundary of the sapphirine–spinel (Spr) and spinel (Spl) fields.

showed that the value of the oxygen activity was 1.5–2 orders of magnitude lower than the magnetite–hematite buffer [Badredinov et al., 2009, Fig. 2]. Thus, the studied spinel–sapphirine reaction structure from metaultramafites of the Aulandzha block is much more oxidized than enderbites and granulites of the Sutam complex. If the spinel–sapphirine model assemblage at 900 °C and 6 kbar is calculated immediately on the MagHem buffer, then the $X_{Fe^{3+}} = Fe^{3+}/(Fe^{3+} + Fe^{2+})$ value in sapphirine will be 0.42. If we obtain the same assemblage with varying fluid composition on the QzFaMag buffer, then the $X_{Fe^{3+}}$ value in sapphirine will be 0.15. As from the data of six analyses (Avchenko et al., 2018, Table 4) the average $X_{Fe^{3+}}$ value in the real sapphirine is 0.41, then a high degree of the sapphirine oxidation in sample 329-5 is quite apparent, and it is similar to the MagHem buffer in the oxygen activity value. A high degree of the sapphirine oxidation in the sample under study is directly (without the thermodynamic calculations) confirmed by the following correlation. In the oxidized rocks of the Wilson Lake terrane 1.7–1.6 Ga in age, Central Labrador, the sap-

Table 4. Comparison of real mineral compositions with model compositions in the Spr + Spl + Pl + Opx + Bt assemblage at 900 °C and 6 kbar

Mineral	Parameter	Real	Model
Spr	X_{mg}	0.89 (average)	0.89
Spl	X_{mg}	0.65 (average)	0.66
Spr	$X_{Fe^{3+}}$	0.41 (average)	0.37
Spl	$X_{Fe^{3+}}$	0.17 (average)	0.16
Bt	X_{mg}	0.83	0.82
Opx	X_{mg}	0.81	0.84
Pl	X_{An}^{Pl}	54–80	63

Note. Fluid composition is given in Table 5.

Table 5. Parameters of fluid composition (partial pressures of gases and logarithm of oxygen fugacity) before the reaction with rock (1) and after it (2)

p_i, bars	p_{CO_2}	p_{CO}	p_{H_2}	p_{CH_4}	p_{H_2O}	$\lg f_{O_2}$
1	4880	134	9	1	972	–13
2	5275	1	0.05	0	724	–8.7

Note. Fluid/rock ratio (W/R) = 0.05.

phirine–quartz assemblage was described in the paragenesis with biotite, perthite K-feldspar, plagioclase, orthopyroxene, magnetite, and titaniferous hematite (Korhonen et al., 2012). By our calculation, the sapphirine from these rocks has the $X_{Fe^{3+}}$ value of 0.51, whereas the Fe_2O_3 content in the titaniferous hematite reaches 1.67 f.u. at the titanium content of 0.16. Thus, the sapphirine from the Wilson Lake terrane, lying almost on the magnetite–hematite buffer, turned out to be more oxidized only in a lower degree than the sapphirine from sample 329-5.

DISCUSSION

Thus, although the studied sapphirine–spinel and garnet gedritites are metaultramafites (Fig. 5), they differ strongly in petrochemistry (Fig. 4) and geochemistry (Figs. 6, 7) from the metaultramafites of the same region and have an oxidation potential that is unusually high for the ancient granulites. Especially interesting is the enrichment of gedritites with Zr, Ba, Rb, Hf, and U as compared with other metaultramafites of the Aulandzha block. For example, the Zr content in sample 329-a is higher than that in sample 325 (which is richer in Zr than other metaultramafites of the Aulandzha block) almost by five times (!). Let us consider the possible explanations of these interesting facts.

The petrological, geochemical, and textural features of these unique rocks (samples 329-a and 329-5) can be explained in three ways: (1) by the protolith hypothesis, (2) by the metasomatic hypothesis, and (3) by the fact that these rocks represent the redeposited crust of weathering of magmatic ultramafites. The first hypothesis suggests that the protolith from which the sapphirine–spinel and garnet gedritites formed was originally enriched in Zr and other components. However, according to the data given in Table 3, such Zr content can be only in alkali granites and syenites, but not in moderately alkaline metaultramafites (Fig. 5). The second hypothesis suggests that the alkaline metasomatism of gedritites was possibly related to the granitization of the Aulandzha block. This hypothesis is supported by Zhulanova. However, this hypothesis contradicts the direct petrographic and geochemical features of these rocks. The matter is that the alkaline metasomatism (one should remember that it is rather intensive alkaline metasomatism) in any case influenced the plagioclase composition – its albitization or origination of more acidic zones of plagioclase on the original more basic cores. However, all observations with the microprobe testify that the plagioclase in gedritites shows the pronounced reverse zoning: It always has acidic cores and a more basic rim, and the difference in composition between the core and rim is significant (56–61 and up to 75–80% An, respectively). At the same time, the alkaline (or acid) metasomatism could not have formed such a zoning of plagioclase. Moreover, in other metaultramafites of the Aulandzha block with a normal content of Zr, Ba, Rb, Hf, and U, and where the metasomatism could not even be suggest-

ed, the plagioclase also shows the reverse zoning. This zoning is, however, well explained (Avchenko et al., 2018) by the evolution of the metamorphism along the regressive *P–T* trend that is accompanied by the supply of the H_2O–CO_2 fluids and superposition of the amphibole with the corresponding redistribution of sodium between amphibole and plagioclase – departure of sodium into amphibole with the formation of the basic marginal zones of plagioclase. This point of view explains the fact of the gedrite contact only with the basic margin of plagioclase (Fig. 3). In addition, it is impossible to explain the high oxidation potential in sample 329-5 from the positions of the alkaline metasomatism, because the common fluids, to which the granitization is related, usually have an oxidation potential somewhere within the quartz–magnetite–fayalite buffer, i.e., significantly lower than in the sapphirine–spinel metaultramafites under consideration. Even the unique finding of the paragenesis of sample 329-5 testifies against the alkaline metasomatism, because the metasomatism related to granitization must have a regional character. Now let us discuss the third hypothesis, according to which the sapphirine–spinel and garnet gedritites represent the redeposited crust of weathering of the magmatic ultramafites. This hypothesis explains well all the features of these rocks and suggests the following scenario of their formation.

In the Paleoproterozoic, the complex of the magmatic ultramafite of the Aulandzha block was exposed onto the Earth's surface, where it underwent weathering, probably underwater one. This process resulted in the formation of the ultrabasic clays of a specific composition and their redeposition accompanied by the mechanical supply of zircons from any source into the fractured zones of the magmatic ultramafites. Then, most likely in the process of the collision metamorphism, which is usually considered the cause of the formation of similar granulitic rocks (Reverdatto et al., 2017), the whole block subsided into the conditions of the high-temperature metamorphism at moderate pressures that resulted in the origination of the metaultramafites — garnet–pyroxene, bipyroxene, and garnet–spinel ones — after the original ultramafites and ultrabasic clays. Then the Aulandzha block was uplifted along the retrograde *P–T* trend (Fig. 8) with the simultaneous supply of the ascending H_2O–CO_2 fluids, garnet disintegration, origination of the reactional structures with sapphirine, orthopyroxene, and gedrite, superposition of amphibole on the early assemblages, and formation of fine zircons 1.9 Ga in age. From this point of view the large zircons with the Paleoarchean cores and oscillatory zoning may have a detrital nature; small zircons, the metamorphogenic one. Zircons of such genesis are not unusual; they were described, for example, in the sapphirine granulites of southwest Norway (Drüppel et al., 2013). However, for the detrital zircons more probable is a significant spread of date that is not observed in a given case: The U–Pb dates of ~3.2 Ga of zircons form a single pronounced cluster in the concordia with the exception of one crystal 2.4 Ga in age (Akinin and Zhulanova, 2016). Although it is

quite possible to explain no spread in the dates of these zircons by the fact that they are supplied from some nearby magmatic source of Paleoarchean age, the problem of the nature of the large zircons – sedimentary-detrital or protomagmatic – requires further study.

If the hypothesis of the metapelite nature of the gedritites under consideration is correct, then the thermodynamic characteristics of the spinel–sapphirine reactional structures may indicate that the oxygen potential on the Earth's surface corresponded to the magnetite–hematite buffer as early as the Paleoproterozoic. This conclusion does not contradict the known sharp increase of the oxygen potential in the early Earth's atmosphere, which is dated at 2.4–2.1 Ga and described as the Great Oxygen Event (GOE) (Lyons et al., 2014). The appearance of the free oxygen in the Earth's atmosphere is connected with the oxygen photosynthesis by the eukaryotes and cyanobacteria, which are diagnosed on the basis of the biomarkers – molecular fossils (Brocks et al., 1999; Rasmussen et al., 2008).

The acceptance of the new original idea of the probable metapelite nature of the sapphirine–spinel and garnet gedritites of the Aulandzha block will require an essential revision of the formation history of the crystalline basement of the OM as a whole. This disputable problem is an interesting task for the future.

CONCLUSIONS

(1) The unique magnesian–aluminous ultrabasic sapphirine–spinel and garnet gedritites of the Aulandzha block strongly differ in petrochemistry and geochemistry from other metaultramafites of the same block. These differences are the enrichment of gedritites in alumina, zirconium, barium, rubidium, hafnium, and uranium and depletion of them in calcium and heavy rare-earth elements. Unusual also is the textural pattern of the gedritite rocks, in which one can see a peculiar banding (lamination?);

(2) The evaluation of the oxidizing potential in the sapphirine–spinel assemblage showed the high oxygen fugacity close to the level of the magnetite–hematite buffer, which was never observed in the ancient granulitic complexes;

(3) The described petrogeochemical features of gedritites of the Aulandzha block are explained by the fact that they are probably the crust of weathering of the enclosing metaultramafites. If this hypothesis is true, then these rocks may indicate that the oxygen potential on the Earth's surface corresponded to the magnetite–hematite buffer as early as the early Proterozoic. This conclusion does not contradict the known Great Oxygen Event on the Earth's surface, which is dated at 2.4–2.1 Ga;

(4) It is not improbable that the large crystals of zircons with the oscillatory zoning and Paleoarchean age of their core zones may are detrital nature, whereas their rims and newly formed fine zircons have the metamorphogenic one.

REFERENCES

Akinin, V.V., Zhulanova, I.L., 2016. Age and geochemistry of zircon from the oldest metamorphic rocks of the Omolon Massif (Northeast Russia). Geochem. Int. 54 (8), 651–659.

Aranovich, L.Ya., Berman, R.G., 1997. A new garnet–orthopyroxene barometer based on reversed Al_2O_3 solubility in $FeO–Al_2O_3–SiO_2$ orthopyroxene. Am. Mineral. 82, 345–353.

Avchenko, O.V., Chudnenko, K.V., Aleksandrov, I.A., 2009. Bases of the Physicochemical Modeling of Mineral Systems [in Russian]. Nauka, Moscow.

Avchenko, O.V., Zhulanova, I.L., Chudnenko, K.V., Karabtsov, A.A., 2018. Spinel–sapphirine reaction structures in the garnet metaultramafic rocks of the Omolon Massif: Petrogenesis and geological interpretation (Northeast Asia). Russ. J. Pac. Geol. 12 (3), 174–189.

Badredinov, Z.G., Sharova, O.I., Avchenko, O.V., Sakhno, V.G., Mishkin, M.A., Vovna, G.M., Karabtsov, A.A., 2009. Magnetite-ilmenite equilibria in Archean enderbites of the Sutam Complex (Aldan shield). Dokl. Earth Sci. 425 (1), 235–238.

Berg, J.H., 1985. Chemical variations in sodium gedrite from Labrador. Am. Mineral. 70 (11–12), 1205–1210.

Bibikova, E.V., 1989. Uranium–lead geochronology of the early stages of development of ancient shields [in Russian]. Nauka, Moscow.

Brocks, J.J., Logan, G.A., Buick, R., Summons, R.E., 1999. Archean molecular fossils and the early rise of eukaryotes. Science 285 (5430), 1033–1036.

Das, K., Fujino, K., Tomioka, N., Miura, H., 2006. Experimental data on Fe and Mg partitioning between coexisting sapphirine and spinel: an empirical geothermometer and its application. Eur. J. Mineral. 18 (1), 49–58.

Diener, J.F.A., Powell, R., White, R.W., Holland, T.J.B., 2007. A new thermodynamic model for clino- and orthoamphiboles in the system $Na_2O–CaO–FeO–MgO–Al_2O_3–SiO_2–H_2O–O$. J. Metamorph. Geol. 25 (6), 631–656.

Drüppel, K., Elsäber, L., Brandt, S., Gerdes, A., 2013. Sveconorwegian mid-crustal ultrahigh-temperature metamorphism in Rogaland, Norway: U-Pb LA-ICP-MS geochronology and pseudosections of sapphirine granulites and associated paragneisses. J. Petrol. 54 (2), 305–350.

Ferry, J.M., Watson, E.B., 2007. New thermodynamic models and revised calibrations for the Ti-in-zircon and Zr-in-rutile thermometers. Contrib. Mineral. Petrol. 154 (4), 429–437.

Gel'man, M.L., 1974. Problems of geology of the ancient metamorphic complexes of the Northeast of the USSR, in: Main Problems of Biostratigraphy and Paleogeography of the Northeast of the USSR [in Russian]. DVNTs AN SSSR, Magadan, pp. 73–79.

Grafchikov, A.A., Fonarev, V.I., 1991. Garnet–orthopyroxene–plagioclase–quartz barometer (experimental calibration), in: Sketches of Physicochemical Petrology [in Russian]. Nauka, Moscow, Issue 16, pp. 199–225.

Green, E., Holland, T., Powell, R., 2007. An order-disorder model for omphacitic pyroxenes in the system jadeite-diopside-hedenbergite-acmite, with applications to eclogitic rocks. Am. Mineral. 92 (7), 1181–1189.

Holland, T.J.B., Powell, R., 1998. An internally consistent thermodynamic data set for phases of petrological interest. J. Metamorph. Geol. 16 (3), 309–343.

Holland, T.J.B., Powell, R., 2011. An improved and extended internally consistent thermodynamic dataset for phases of petrological interest, involving a new equation of state for solids. J. Metamorph. Geol. 29 (3), 333–383.

Kelsey, D.E., Hand, M., 2015. On ultrahigh temperature crustal metamorphism: Phase equilibria, trace element thermometry, bulk composition, heat sources, timescales and tectonic settings. Geosci. Front. 6 (3), 311–356.

Kogarko, L.N., Lazutkina, L.N., Krigman, L.D., 1988. Conditions of Zircon Concentration in the Magmatic Processes [in Russian]. Nauka, Moscow.

Korhonen, F.J., Powell, R., Stout, J.H., 2012. Stability of sapphirine + quartz in the oxidized rocks of the Wilson Lake terrane, Labrador: calculated equilibria in NCKFMASHTO. J. Metamorph. Geol. 30, 21–36.

Kotlyar, I.N., Zhulanova, I.L., Rusakova, T.B., Gagieva, A.M., 2001. Isotope Systems of Magmatic and Metamorphic Complexes of Northeast Russia [in Russian]. SVKNII DVO RAN, Magadan.

Kriegsman, L.M., Schumacher, J.C., 1999. Petrology of sapphirine-bearing and associated granulites from central Sri Lanka. J. Petrol. 40 (8), 1211–1239.

Lavrent'eva, I.V., Perchuk, L.L., 1991. Experimental study of the phase correlation in the garnet–orthopyroxene–amphibole system at 700 and 800 °C, in: Sketches of Physicochemical Petrology [in Russian], Part XVI. Nauka, Moscow, pp. 139–164.

Lee, B.I., Kesler, M.G., 1975. A generalized thermodynamic correlation based on three-parameter corresponding states. AIChE J. 21 (3), 510–527.

Lyons, T.W., Reinhard, C.T., Planavsky, N.J., 2014. The rise of oxygen in Earth's early ocean and atmosphere. Nature 506 (7488), 307–315.

McDonough, W.F., Sun, S.-S., 1995. The composition of the Earth. Chem. Geol. 120 (3–4), 223–253.

Owen, J.V., Greenough, J.D., 1991. An empirical sapphirine-spinel Mg-Fe exchange thermometer and its application to high grade xenoliths in the Popes Harbour dyke, Nova Scotia, Canada. Lithos 26 (3–4), 317–332.

Rasmussen, B., Fletcher, I.R., Brocks, J.J., Kilburn, M.R., 2008. Reassessing the first appearance of eukaryotes and cyanobacteria. Nature 455, 1101–1104.

Reverdatto, V.V., Likhanov, I.I., Polyansky, O.P., Sheplev, V.S., Kolobov, V.Yu., 2017. Nature and Models of Metamorphism [in Russian]. Izd. SO RAN, Novosibirsk.

Sato, K., Miyamoto, T., Kawasaki, T., 2006. Experimental calibration of sapphirine–spinel Fe^{2+}–Mg exchange thermometer: Implication for constraints on *P–T* condition of Howard Hills, Napier Complex, East Antarctica. Gondwana Res. 9 (4), 398–408.

Sharpenok, L.P. (Ed.), 2009. Petrographic Code of Russia. Magmatic, Metamorphic, Metasomatic, and Impact Formations [in Russian], VSEGEI, St. Petersburg.

Steffen, G., Seifert, F., Amthauer, G., 1984. Ferric iron in sapphirine: a Mössbauer spectroscopic study. Am. Mineral. 69 (3), 339–348.

Tajčmanová, L., Connolly, J.A.D., Cesare, B., 2009. A thermodynamic model for titanium and ferric iron solution in biotite. J. Metamorph. Geol. 27 (2), 153–165.

Taylor-Jones, K.A., Powell, R.P., 2010. The stability of sapphirine + quartz: calculated phase equilibria in $FeO–MgO–Al_2O_3–SiO_2–TiO_2–O$. J. Metamorph. Geol. 28 (6), 615–633.

Wheller, C.J., Powell, R., 2014. A new thermodynamic model for sapphirine: calculated phase equilibria in $K_2O–FeO–MgO–Al_2O_3–SiO_2–H_2O–TiO_2–Fe_2O_3$. J. Metamorph. Geol. 32 (3), 287–299.

White, R.W., Powell, R., Clarke, G.L., 2002. The interpretation of reaction textures in Fe-rich metapelitic granulites of the Musgrave Block, central Australia: constraints from mineral equilibria calculations in the system $K_2O–FeO–MgO–Al_2O_3–SiO_2–H_2O–TiO_2–Fe_2O_3$. J. Metamorph. Geol. 20 (1), 41–55.

White, R.W., Pomroy, N.E., Powell, R., 2005. An in situ metatexite–diatexite transition in upper amphibolite facies rocks from Broken Hill, Australia. J. Metamorph. Geol. 23 (7), 579–602.

Whitney, D.L., Evans, B.W., 2010. Abbreviations for names of rock-forming minerals. Am. Mineral. 95 (1), 185–187.

Zhulanova, I.L., 1990. The Earth's Crust of Northeast Asia in the Precambrian and Phanerozoic Time [in Russian]. Nauka, Moscow.

Zhulanova, I.L., Avchenko, O.V., Sharova, O.I., 2014. The garnet ultramafics and garnet gedritites of the Omolon microcontinent: deep diaphthoresis with geologic and tectonic interpretation. Fundam. Res. 8 (6), 1393–1399.

Editorial responsibility: V.S. Shatsky